Adaptive Beamforming of Vertical Frequency Diverse Array for Airborne Radar

Xuzi Wu(✉) and Yongliang Sun

School of Computer Science and Technology,
Nanjing Tech University, Nanjing 211816, China
xuziwu@njtech.edu.cn

Abstract. To decouple the range-angle-dependent beampattern, a new type of frequency diverse array (FDA) with frequency increment applied across the vertical array elements is proposed, referred to as the vertical frequency diverse array (VFDA). The adaptive algorithm for the design of the receive antenna is also presented to generate a single-maximum beampattern. Simulation results verify the effectiveness. It shows that the proposed approach outperforms the multiple-input multiple-output (MIMO) radar in focusing the transmit energy on the far-field targets.

Keywords: Beamforming · Frequency diverse array · Range-dependent

1 Introduction

Phased-array has been widely used in airborne radar systems for its flexible beam scanning ability. However, the beampattern of the phased-array is range independent. When detecting the ground moving targets, the transmit energy would be distributed broadly in range with the decrease of the elevation angle, resulting in more mainlobe interference. To achieve narrow mainlobe, the enlarged antenna aperture is needed, which is however difficult for the radar with limited antenna size. To overcome this disadvantage, a novel beam scanning array, referred to as the FDA, was presented in [1]. Benefits have been demonstrated by applying the unique range-dependent characteristic of the FDA to different radar tasks, e.g. target localization [2, 3], clutter suppression [4, 5], pattern synthesis [6–9]. In the conventional FDA, a linear frequency increment is always applied across the horizontal elements of the antenna array, providing an increased degrees-of-freedom (DOFs) to design and control the beampattern. However, it may be difficult to implement in actual airborne radar systems due to the range-angle-coupling and time-variant effects on the estimate of the effective covariance matrix.

To decouple the range-angle dependent beampattern, a nonuniform linear array was employed in [7], which may be difficult to implement due to the high accuracy requirement of the transmitter and receiver positions. A logarithmically increasing frequency increment was proposed in [8] to synthesize a nonperiodic beampattern. But it is unable to obtain the closed form expression of the beampattern. In [9], the convex optimization is used to achieve dot-shaped transmit beampattern and better resolution

S. Han et al. (Eds.): AICON 2019, LNICST 286, pp. 203–209, 2019.
https://doi.org/10.1007/978-3-030-22968-9_18

in the range dimension compared with that in [8]. However, the algorithm has a relatively high complexity, which is difficult for the implementation of the multilog-FDA.

In this paper, a new type of FDA with frequency increment used across the vertical array elements is explored. The design algorithm for the receive array configuration is also presented to generate a beampattern with no grating lobes. Compared to the beampattern in the conventional FDA and the MIMO radar, the single-maximum and range-dependent beampattern in the VFDA may be more capable of rejecting clutter and jamming in airborne radar systems.

2 Adaptive Beamforming Algorithm

2.1 The Transmit Beampattern of VFDA

Consider an $(M \times N)$-element planar array antenna with uniform frequency increment Δf across the vertical elements, the signal transmitted by the (m, n)th element is

$$s_{m,n}(t) = \exp(j2\pi f_m t) = \exp\{j2\pi[f_0 + (m-1)\Delta f]t\} \tag{1}$$

where f_0 is the carrier frequency. For a far-field point target located at the azimuth angle φ, elevation angle θ, and range R relative to the (0, 0)th element, the signal arriving at the target can be expressed as

$$s_{m,n}(t - R_{m,n}/c) = \alpha_{m,n}\exp\{j2\pi f_m(t - R_{m,n}/c)\} \tag{2}$$

where c is the speed of light, $\alpha_{m,n}$ is a complex weighting factor that represents transmission and propagation effects.

$$R_{m,n} = R - (n-1)d_N \cos\ \theta \cos \varphi + (m-1)d_M \sin\ \theta \tag{3}$$

is the range of the target to the (m, n)th element with d_M and d_N representing the vertical and horizontal element spacing, respectively. Taking the narrowband assumption, the VFDA transmit beampattern steered to $(\theta_0, \varphi_0, R_0)$ is given by

$$\begin{aligned} G_t(t,\theta,\varphi,R) = &\sum_{m=1}^{M}\sum_{n=1}^{N}\alpha_{m,n} \exp\left[j2\pi f_m\left(t - \frac{R_{m,n}}{c}\right)\right] \cdot \exp\left[j2\pi f_m \frac{R_0}{c}\right] \\ &\cdot\exp\left[-j2\pi f_m(n-1)\cos\theta_0 \cos\varphi_0 \frac{d_N}{c}\right] \cdot \exp\left[j2\pi f_m(m-1)\sin\ \theta_0 \frac{d_M}{c}\right] \end{aligned} \tag{4}$$

The approximated expression of $|G_t(t,\theta,\varphi,R)|$ is

$$|G_t(t,\theta,\varphi,R)| \approx \left|\frac{\sin[\pi N(\cos\ \theta \cos\ \varphi - \cos\ \theta_0 \cos\ \varphi_0)d_N/\lambda_0]}{\sin[\pi(\cos\ \theta \cos\ \varphi - \cos\ \theta_0 \cos\ \varphi_0)d_N/\lambda_0]}\right| \cdot \left|\frac{\sin[\pi M\Delta ft - \pi M\Delta f(R-R_0)/c - \pi M(\sin\ \theta - \sin\ \theta_0)d_M/\lambda_0]}{\sin[\pi\Delta ft - \pi\Delta f(R-R_0)/c - \pi(\sin\ \theta - \sin\ \theta_0)d_M/\lambda_0]}\right| \tag{5}$$

where $\lambda_0 = c/f_0$. Here we have assumed that the complex weighting factors are all equal to 1,

$$(M-1)\Delta f \ll f_0 \tag{6}$$

and

$$R \gg \max\left[(M-1)^2 d_M/\lambda_0, (M-1)(N-1)d_N/\lambda_0\right] \tag{7}$$

It can be observed that the phase differences depending on time and range are incorporated into the second term of (5), positioning the multiple maxima at different ranges but the same azimuth angle φ_0. Therefore, the pattern will not keep the 'S'-shaped feature with coupling between the azimuth angle and range. The following task is to synthesize the beampattern with no grating lobes in the range dimension.

2.2 Transmit-Receive Beamforming with no Grating Lobes

A $(Q \times P)$-element receive array collocated with the transmit antenna is considered in this paper. When the signal is received by each element, a set of bandpass filters will be applied to extract the complete transmit signals. We then have the VFDA two-way beampattern

$$\begin{aligned} G_r(t,\theta,\varphi,R) = &\sum_{q=1}^{Q}\sum_{p=1}^{P}\sum_{m=1}^{M}\sum_{n=1}^{N}\exp\left[j2\pi f_m\left(t - \frac{R_{m,n}+R_{q,p}}{c}\right)\right] \\ &\cdot \exp\left[j4\pi f_m \frac{R_0}{c}\right] \cdot \exp\left[-j2\pi f_m(n-1)\cos\ \theta_0 \cos\ \varphi_0 \frac{d_N}{c}\right] \\ &\cdot \exp\left[-j2\pi f_m(p-1)\cos\ \theta_0 \cos\ \varphi_0 \frac{d_P}{c}\right] \\ &\cdot \exp\left[j2\pi f_m(m-1)\sin\ \theta_0 \frac{d_M}{c}\right] \cdot \exp\left[j2\pi f_m(q-1)\sin\ \theta_0 \frac{d_Q}{c}\right] \end{aligned} \tag{8}$$

where $R_{q,p}$ is the range of the target to the (q, p)th receive element. d_Q and d_P are the vertical and horizontal element spacing in the receiver, respectively. Assume $P = N$ and $d_P = d_N$, $|G_r(t,\theta,\varphi,R)|$ can be simplified as

$$
\begin{aligned}
&|G_r(t,\theta,\varphi,R)| \\
&\approx \left|\frac{\sin[\pi N(\cos\theta\cos\varphi-\cos\theta_0\cos\varphi_0)d_N/\lambda_0]}{\sin[\pi(\cos\theta\cos\varphi-\cos\theta_0\cos\varphi_0)d_N/\lambda_0]}\right|^2 \\
&\cdot\left|\frac{\sin[\pi M\Delta ft-2\pi M\Delta f(R-R_0)/c-\pi M(\sin\ \theta-\sin\ \theta_0)d_M/\lambda_0]}{\sin[\pi\Delta ft-2\pi\Delta f(R-R_0)/c-\pi(\sin\ \theta-\sin\ \theta_0)d_M/\lambda_0]}\right| \\
&\cdot\left|\frac{\sin\left[\pi Q(\sin\ \theta-\sin\ \theta_0)d_Q/\lambda_0\right]}{\sin\left[\pi(\sin\ \theta-\sin\ \theta_0)d_Q/\lambda_0\right]}\right|
\end{aligned}
\quad (9)
$$

In order to avoid the grating lobes in the range dimension, the adaptive beamforming algorithm is presented in the following procedure.

Step 1: Ignore the effect of the earth curvature, the maxima of the second term in (9) can be achieved when the phase term satisfies

$$
\pi\Delta ft-2\pi\Delta f(R-R_0)/c-\pi(R/H-R_0/H)d_M/\lambda_0=a\pi \quad (10)
$$

where a is an integer and H is the platform altitude. Thus, the grating lobes are located at

$$
\bar{R}=\frac{\eta+\sqrt{\eta^2-8c\Delta fHd_M/\lambda_0}}{4\Delta f};\ \bar{R}\in[H,R_{\max}],\ a\neq 0 \quad (11)
$$

where $R_{\max}$ is the maximum range of radar.

$$
\eta=c\Delta ft+2\Delta fR_0-ac+cHd_M/R_0\lambda_0 \quad (12)
$$

Define

$$
\sigma=|H/\bar{R}-H/R_0| \quad (13)
$$

and calculate the maximum and minimum value of (13) as $\sigma_{\max}$ and $\sigma_{\min}$, respectively.

Step 2: For the last term of (9), the pattern peaks are separated by λ_0/d_Q. To avoid the furthest grating lobe from moving into the peaks, we require

$$
\lambda_0/d_Q\geq\sigma_{\max}+\sigma_{\min} \quad (14)
$$

Then, the vertical element spacing d_Q in the receiver should be constrained to

$$
0<d_Q\leq\lambda_0/(\sigma_{\max}+\sigma_{\min}) \quad (15)
$$

Step 3: Fix d_Q, the beamwidth of the last term in (9) is

$$B_r = 2\lambda_0 / Q d_Q \tag{16}$$

To ensure the nearest grating lobe outside of the main beam, the number of the vertical array elements Q should satisfy

$$B_r = 2\lambda_0 / Q d_Q \leq \sigma_{\min} \tag{17}$$

This can be rewritten as

$$Q \geq \text{ceil}\left[\lambda_0 / (d_Q \sigma_{\min})\right] \tag{18}$$

where $\text{ceil}[\cdot]$ denotes the nearest integer towards infinity.

3 Simulation Results

In the simulations, an X-band VFDA radar operating at a carrier frequency of $f_0 = 10$ GHz is simulated. The transmit antenna is set with 8×8 elements and the element space is $d_M = d_N = 0.015$ m. The frequency increment is taken as $\Delta f = 2$ KHz. The platform altitude and radar maximum range are $H = 8$ km and $R_{\max} = 300$ km, respectively. Assume the target is positioned at $(2°, 90°, 229\text{ km})$, it is calculated that there are 2 maxima in the range of (8 km, 300 km) except R_0. The maximum and minimum value of σ are $\sigma_{\max} = 58 \times 10^{-3}$ and $\sigma_{\min} = 16 \times 10^{-3}$, respectively. Based on (14) and (15), the receive antenna is designed with $Q = 6$ vertical array elements and $d_Q = 0.35$ m element space.

Assume $t = 0$, Fig. 1 shows the comparison of the normalized beampatterns generated by the MIMO radar and the VFDA radar, respectively. In Fig. 1(a), it can be observed that the mainlobe is seriously expanded in the range dimension due to the small value of φ_0. For the VFDA, the beamwidth of the pattern is range-dependent and a function of the frequency increment Δf and the number of the vertical array elements M. This generates a different beampattern with energy distributed in smaller range regions, as is shown in Fig. 1(b). By using the proposed algorithm for antenna design, the beampattern with no grating lobes is synthesised in Fig. 1(c). It can be noticed that the azimuth angle of the mainlobe in the VFDA is constant along the range axis, which is different from that in the conventional FDA. This avoids the coupling between angle and range, therefore, is a more capable approach to reject the range-dependent interference and improve the signal-to-interference-plus-noise (SINR) ratio.

4 Conclusion

An Adaptive transmit-receive beamforming algorithm for the VFDA has been proposed to decouple the range-angle-dependent beampattern and suppress the grating lobes in the range dimension. Simulation results show that the proposed approach performs better in focusing the transmit energy on the desired targets, especially in the far-field ranges. And the low complexity of the algorithm is also suitable for the

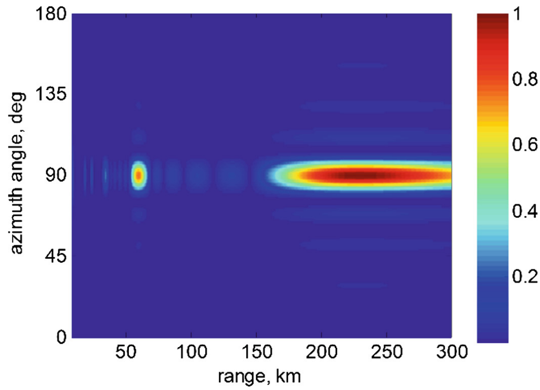

(a)

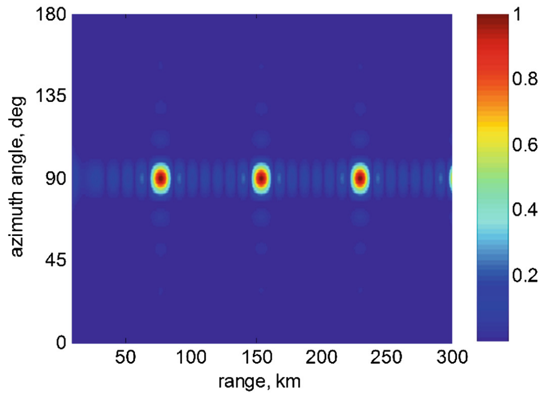

(b)

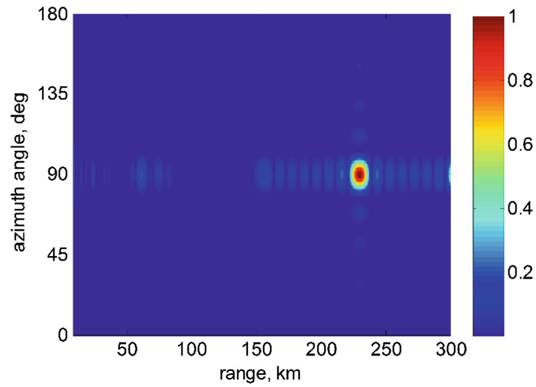

(c)

Fig. 1. Comparison of the normalized transmit-receive beampatterns: (a) MIMO radar with $Q = 6$ and $d_Q = 0.35$ m; (b) VFDA radar with no antenna design where $Q = 6$ and $d_Q = 0.015$ m; (c) VFDA radar with $Q = 6$ and $d_Q = 0.35$ m.

implementation of the VFDA in practice. However, the beampattern of the VFDA is still time-variant, similar to that of the conventional FDA, which is reserved for subsequent research.

References

1. Antonik, P., Wicks, M.C., Griffiths, H.D., et al.: Frequency diverse array radars. In: Proceedings of the IEEE Radar Conference, Verona, pp. 215–217 (2006)
2. Wang, W.-Q., So, H.C.: Transmit subaperturing for range and angle estimation in frequency diverse array radar. IEEE Trans. Sig. Process. **62**(8), 2000–2011 (2014)
3. Wang, W.-Q., Shao, H.: Range-angle localization of targets by a double-pulse frequency diverse array radar. IEEE J. Sel. Top. Sig. Process. **8**(1), 106–114 (2014)
4. Baizert, P., Hale, T.B., Temple, M.A., et al.: Forward-looking radar GMTI benefits using a linear frequency diverse array. Electron. Lett. **42**(22), 1311–1312 (2006)
5. Xu, J., Zhu, S., Liao, G.: Range ambiguous clutter suppression for airborne FDA-STAP radar. IEEE J. Sel. Top. Sig. Process. **9**(8), 1620–1631 (2015)
6. Wang, W.-Q.: Cognitive frequency diverse array radar with situational awareness. IET Radar Sonar Navig. **10**(2), 359–369 (2016)
7. Sammartino, P.F., Baker, C.J., Griffiths, H.D.: Frequency diverse MIMO techniques for radar. IEEE Trans. Aerosp. Electron. Syst. **49**(1), 201–222 (2013)
8. Khan, W., Qureshi, I.M., Saeed, S.: Frequency diverse array radar with logarithmically increasing frequency offset. IEEE Antennas Wirel. Propag. Lett. **14**, 499–502 (2015)
9. Shao, H., Dai, J., Xiong, J., et al.: Dot-shaped range-angle beampattern synthesis of frequency diverse array. IEEE Antennas Wirel. Propag. Lett. **15**, 1703–1706 (2016)